ELSEVIER

Global Bayesian Analysis of the Higgs-boson Couplings☆

Jorge de Blas[a], Marco Ciuchini[b], Enrico Franco[a], Diptimoy Ghosh[a], Satoshi Mishima[c,d], Maurizio Pierini[e], Laura Reina[f], Luca Silvestrini[a]

[a]*INFN, Sezione di Roma, Piazzale A. Moro 2, I-00185 Roma, Italy*
[b]*INFN, Sezione di Roma Tre, Via della Vasca Navale 84, I-00146 Roma, Italy*
[c]*Dipartimento di Fisica, Università di Roma "La Sapienza", Piazzale A. Moro 2, I-00185 Roma, Italy*
[d]*SISSA, Via Bonomea 265, I-34136 Trieste, Italy*
[e]*California Institute of Technology, Pasadena, California, USA*
[f]*Physics Department, Florida State University, Tallahassee, FL 32306-4350, USA*

Abstract

We present preliminary results of a bayesian fit to the Wilson coefficients of the Standard Model gauge invariant dimension-6 operators involving one or more Higgs fields, using data on electroweak precision observables and Higgs boson signal strengths.

Keywords: Higgs boson, Effective field theory

1. Introduction

After a decades-long hunt, in the summer of 2012 the physics world erupted in excitement when both the AT-LAS and CMS experiments at the Large Hadron Collider (LHC) at CERN announced their discovery of a particle that looked like the Higgs boson (H) [1, 2]. With the help of two-and-a-half times more data and sophisticated experimental analyses, it is now confirmed that the newfound particle behaves, indeed, very much like the Standard Model (SM) Higgs boson. That this Higgs boson decays to SM gauge bosons is now established with high statistical significance. In fact, each of

the decay channels $H \to \gamma\gamma$, $H \to W^+W^-$ and $H \to ZZ$ is by now a discovery channel. There is also good evidence of its non-universal couplings to fermions. The decays to $\tau^+\tau^-$ and $b\bar{b}$ final states have also been seen with good confidence.

Since the Higgs-boson mass (m_H) has now been measured, its couplings to SM particles are completely predicted except for the residual arbitrariness introduced by the Yukawa couplings to fermions, which are nevertheless very constrained by the precise measurement of fermion masses. This means that any deviation from the SM predictions will provide unambiguous evidence for New Physics (NP). Unfortunately, large deviations from the SM expectations are already ruled out (except possibly in the couplings to light fermions and/or $H \to Z\gamma$). This, in conjunction with the absence of any other direct NP signal so far, leads us to expect a deviation at the level of no more than a few percents. Hence, a rigorous study of the Higgs-boson couplings in the Run-II of the LHC and also in the high luminosity phase is mandatory.

Although new particles at the TeV scale or below are perfectly allowed by the LHC data, it is interesting to study the sensitivity of the current Higgs-boson

related measurements to short-distance physics assuming an effective field theory framework. The effect of heavy NP (beyond the reach of LHC for direct production) can be parametrized in terms of gauge-invariant higher-dimensional operators involving only SM fields. In this case, one supplements the SM Lagrangian with operators of mass dimension greater than 4,

$$\mathcal{L} = \mathcal{L}_{\rm SM} + \frac{1}{\Lambda}\mathcal{L}^{(5)} + \frac{1}{\Lambda^2}\mathcal{L}^{(6)} + .. \tag{1}$$

In the SM there is only one operator of dimension 5, the celebrated Weinberg operator which gives Majorana masses to light neutrinos [3]. As this operator is irrelevant for our discussion of Higgs physics, we will not consider it here. On the other hand, the number of dimension-6 operators is much higher: even for one generation the count of the total number of operators grows to 59 [4] [1]. Adding general flavour structure increases this number to a gigantic 2499 [6]. For phenomenological explorations of some of these operators and related studies, see [7, 8, 9, 10, 11, 12, 13, 14, 15, 16, 17, 18, 19, 20, 21, 6, 22, 23, 24, 25, 26, 27, 28, 29, 30, 31, 32, 33, 34, 35, 36].

In the following section we will choose one operator basis and introduce the set of operators considered in this work. The experimental data used in our analysis will be discussed in Sec. 3. We will present our results in Sec. 4 and outline some conluding remaks in Sec. 5.

2. Operator basis

Several operator bases have been used in the literature to describe the physics of gauge-invariant dimension-6 operators in the SM [37, 38, 4]. In this work we concentrate on electroweak and Higgs-boson observables only. While depending on the set of observables chosen for a specific study one of these operator bases can be more convenient than others, physics should be basis independent. Moreover, we aim to study also other observables (e.g., flavour and other low-energy ones) in the near future. Therefore the choice of one operator basis is as good as any other one for our purpose. As we do not want to introduce another new basis in the literature, we choose to adopt the fairly general basis introduced in Ref. [4]. As mentioned earlier, the total number of independent operators was shown to be

59. The basis of Ref. [4] consists of 15 bosonic operators, 19 single-fermionic-current operators and 25 four-fermion operators for each fermion generation. Since in this study we limit ourselves to electroweak and Higgs-boson signal strength observables (extending the previous work by some of us [8, 28, 32]), we consider only a subset of operators. In particular, we only consider operators involving one or more Higgs fields. Operators which involve fermionic fields are assumed to be flavour-diagonal and family universal. Moreover, we restrict this study to Charge-Parity (CP) even operators only. As the Wilson coefficients are generated at the scale Λ, ideally, one should also use the Renormalization Group Equations (RGE) to evolve them from the scale Λ to the energy scale relevant for the process of interest[2]. In this work we neglect the effect of RGE. Below, we introduce our notations and list all the operators relevant for our study.

- Bosonic operators:

$$O_{HG} = (H^\dagger H)G^A_{\mu\nu}G^{A\mu\nu} , \tag{2}$$
$$O_{HW} = (H^\dagger H)W^I_{\mu\nu}W^{I\mu\nu} , \tag{3}$$
$$O_{HB} = (H^\dagger H)B_{\mu\nu}B^{\mu\nu} , \tag{4}$$
$$O_{HWB} = (H^\dagger\tau^I H)W^I_{\mu\nu}B^{\mu\nu} , \tag{5}$$
$$O_{HD} = (H^\dagger D^\mu H)^*(H^\dagger D_\mu H) , \tag{6}$$

where τ^I are the three Pauli matrices.

The Wilson coefficients for the operators O_{HWB} and O_{HD} (we denote them by C_{HWB} and C_{HD} respectively) are related to the well known Peskin and Takeuchi parameters S and T [39] by,

$$S = \frac{4s_W c_W}{\alpha_{\rm em}(M_Z)}\frac{{\rm v}^2}{\Lambda^2}C_{HWB} , \tag{7}$$
$$T = -\frac{1}{2\alpha_{\rm em}(M_Z)}\frac{{\rm v}^2}{\Lambda^2}C_{HD} , \tag{8}$$

where c_W and s_W are the cosine and sine of the weak mixing angle θ_W respectively, v is the Vacuum Expectation Value (VEV) of the Higgs field and $\alpha_{\rm em}$ is the electromagnetic fine-structure constant.

In addition to the above operators, there are two more purely bosonic operators involving only the Higgs-boson field, namely,

$$O_{H\square} = (H^\dagger H)\square(H^\dagger H) \text{ and} \tag{9}$$
$$O_H = (H^\dagger H)^3 . \tag{10}$$

[1]The original work by Buchmuller and Wyler [5] had 80 operators out of which only 59 were shown to be independent by the authors of [4].

[2]The anomalous dimension matrix for all the 2499 operators has been computed recently in [20, 21, 6].

The operator $O_{H\square}$ contributes to the wave-function renormalization of the Higgs field and O_H contributes to the Higgs potential, i.e., the VEV v and the SM Higgs-boson self coupling λ. We will see later that this makes $O_{H\square}$ poorly constrained and O_H, which does not affect our observables at all, remains unconstrained by our analysis. A joint measurement of the Higgs mass m_H and the self-coupling λ is required to constrain this operator. There are 8 more bosonic operators (6 CP odd + 2 CP even) in the total 15 bosonic operators listed in [4], but they either do not involve any Higgs field or are CP-odd. Thus, we do not consider them in our analysis.

- Single-fermionic-current operators:

$$O_{HL}^{(1)} = (H^\dagger i \overleftrightarrow{D}_\mu H)(\bar{L}\gamma^\mu L) , \qquad (11)$$

$$O_{HL}^{(3)} = (H^\dagger i \overleftrightarrow{D}_\mu^I H)(\bar{L}\tau^I\gamma^\mu L) , \qquad (12)$$

$$O_{He} = (H^\dagger i \overleftrightarrow{D}_\mu H)(\bar{e}_R\gamma^\mu e_R) , \qquad (13)$$

$$O_{HQ}^{(1)} = (H^\dagger i \overleftrightarrow{D}_\mu H)(\bar{Q}\gamma^\mu Q) , \qquad (14)$$

$$O_{HQ}^{(3)} = (H^\dagger i \overleftrightarrow{D}_\mu^I H)(\bar{Q}\tau^I\gamma^\mu Q) , \qquad (15)$$

$$O_{Hu} = (H^\dagger i \overleftrightarrow{D}_\mu H)(\bar{u}_R\gamma^\mu u_R) , \qquad (16)$$

$$O_{Hd} = (H^\dagger i \overleftrightarrow{D}_\mu H)(\bar{d}_R\gamma^\mu d_R) , \qquad (17)$$

$$O_{Hud} = i(\widetilde{H}^\dagger D_\mu H)(\bar{u}_R\gamma^\mu d_R) . \qquad (18)$$

As we consider flavour diagonal couplings only, all the above operators except O_{Hud} are hermitian. Here, $\widetilde{H} = i\tau^2 H^*$ and the hermitian derivatives have been defined as,

$$H^\dagger \overleftrightarrow{D}_\mu H = H^\dagger(D_\mu H) - (D_\mu H)^\dagger H \text{ and} \qquad (19)$$

$$H^\dagger \overleftrightarrow{D}_\mu^I H = H^\dagger \tau^I(D_\mu H) - (D_\mu H)^\dagger \tau^I H . \qquad (20)$$

There are also (non-hermitian) operators involving scalar fermionic currents,

$$O_{eH} = (H^\dagger H)(\bar{L} e_R H) , \qquad (21)$$

$$O_{uH} = (H^\dagger H)(\bar{Q} u_R \widetilde{H}) , \qquad (22)$$

$$O_{dH} = (H^\dagger H)(\bar{Q} d_R H) . \qquad (23)$$

Once the Higgs field gets a VEV, these operators modify the SM Yukawa couplings. There are 8 more operator structures which involve tensor fermionic currents. We do not consider them in the analysis presented here.

3. Experimental data

In order to constrain the Wilson coefficients of the dimension-6 operators induced by NP, we use the data on (1) ElectroWeak Precision Observables (EWPO) from SLD, LEP-I, LEP-II and Tevatron and (2) Higgs signal strengths from ATLAS and CMS. The experimental values of the EWPO are summarized in Table 1.

$\alpha_s(M_Z^2)$	0.1185 ± 0.0005
$\Delta\alpha_{\text{had}}^{(5)}(M_Z^2)$	0.02750 ± 0.00033
M_Z [GeV]	91.1875 ± 0.0021
m_t [GeV]	173.34 ± 0.76
m_H [GeV]	125.5 ± 0.3
M_W [GeV]	80.385 ± 0.015
Γ_W [GeV]	2.085 ± 0.042
Γ_Z [GeV]	2.4952 ± 0.0023
σ_h^0 [nb]	41.540 ± 0.037
$\sin^2\theta_{\text{eff}}^{\text{lept}}(Q_{\text{FB}}^{\text{had}})$	0.2324 ± 0.0012
P_τ^{pol}	0.1465 ± 0.0033
$\mathcal{A}_\ell$ (SLD)	0.1513 ± 0.0021
$\mathcal{A}_c$	0.670 ± 0.027
$\mathcal{A}_b$	0.923 ± 0.020
$A_{\text{FB}}^{0,\ell}$	0.0171 ± 0.0010
$A_{\text{FB}}^{0,c}$	0.0707 ± 0.0035
$A_{\text{FB}}^{0,b}$	0.0992 ± 0.0016
R_ℓ^0	20.767 ± 0.025
R_c^0	0.1721 ± 0.0030
R_b^0	0.21629 ± 0.00066

Table 1: Summary of experimental data on EWPO.

For the definitions and theoretical expressions of the EWPO and related issues, we refer the reader to [28] and the references therein [3]. The quantities in the first five rows in Table 1 have been used as inputs of our fit. Currently, we have used only their central values while fitting the NP coefficients.

In addition to the EWPO, we also use the data on Higgs signal strengths from the ATLAS and CMS experiments. The theory prediction for the signal strength μ of one specific analysis can be computed as,

$$\mu = \sum_i w_i r_i , \qquad (24)$$

where the sum runs over all the channels which can contribute to the final state of the analysis. The individual channel signal strength r_i and the SM weight for that

---

[3]For an update of their analysis see [40].

Coefficient	Only EW C_i/Λ^2 [TeV^{-2}] at 95%	Only Higgs C_i/Λ^2 [TeV^{-2}] at 95%	EW + Higgs C_i/Λ^2 [TeV^{-2}] at 95%
C_{HG}	$--$	$[-0.0077, 0.0066]$	$[-0.0077, 0.0066]$
C_{HW}	$--$	$[-0.039, 0.012]$	$[-0.039, 0.012]$
C_{HB}	$--$	$[-0.011, 0.003]$	$[-0.011, 0.003]$
C_{HWB}	$[-0.0082, 0.0030]$	$[-0.006, 0.020]$	$[-0.0063, 0.0039]$
C_{HD}	$[-0.025, 0.004]$	$[-4.0, 1.4]$	$[-0.025, 0.004]$
$C_{H\square}$		$[-1.2, 2.0]$	$[-1.2, 2.0]$
$C_{HL}^{(1)}$	$[-0.005, 0.012]$	$--$	$[-0.005, 0.012]$
$C_{HL}^{(3)}$	$[-0.010, 0.005]$	$[-1.2, 0.3]$	$[-0.010, 0.005]$
C_{He}	$[-0.015, 0.006]$	$--$	$[-0.015, 0.006]$
$C_{HQ}^{(1)}$	$[-0.026, 0.041]$	$[-28, 15]$	$[-0.026, 0.041]$
$C_{HQ}^{(3)}$	$[-0.011, 0.013]$	$[-0.6, 2.2]$	$[-0.011, 0.013]$
C_{Hu}	$[-0.067, 0.077]$	$[-5, 11]$	$[-0.067, 0.077]$
C_{Hd}	$[-0.14, 0.06]$	$[-33, 15]$	$[-0.14, 0.06]$
C_{Hud}	$--$	$--$	$--$
C_{eH}	$--$	$[-0.071, 0.024]$	$[-0.071, 0.024]$
C_{uH}	$--$	$[-0.50, 0.59]$	$[-0.50, 0.59]$
C_{dH}	$--$	$[-0.073, 0.078]$	$[-0.072, 0.078]$

Table 2: Fit results for the coefficients of the dimension six operators at 95% probability. The fit is performed switching on one operator at a time. Bounds from only EWPO, only Higgs signal strengths and the combined ones are shown separately.

channel w_i are defined as

$$r_i = \frac{[\sigma \times BR]_i}{[\sigma_{SM} \times BR_{SM}]_i} \text{ and} \qquad (25)$$

$$w_i = \frac{\epsilon_i [\sigma_{SM} \times BR_{SM}]_i}{\sum_j \epsilon_j^{SM} [\sigma_{SM} \times BR_{SM}]_j} . \qquad (26)$$

In the presence of NP the relative experimental efficiencies, ϵ_i, will in general be different from their values in the SM. In particular, the appearance of new tensor structures in the vertices can modify the kinematic distribution of the final-state particles, thereby changing the efficiencies. In this work, we assume that this effect is negligible and use the SM weight factors throughout. This assumption is valid for small deviations from the SM couplings so that kinematic distributions are not changed significantly.

We have implemented our effective Lagrangian in FeynRules [41] and used Madgraph [42] to compute the NP contributions to the Higgs production cross sections numerically at the tree level. In order to compute the branching ratios we have used the formulae given in [25] after changing them to our basis. We only consider NP effects which are linear ($O(1/\Lambda^2)$) in the dimension-6 operator coefficients. In all cases, the SM K-factors[4]

have been used to estimate the effect of QCD corrections, even for the NP contributions. No theoretical uncertainties have been associated to the cross sections and branching ratios in our current analysis.

Experimental measurements for the signal strengths have been taken from Refs. [44, 45] for $H \to \gamma\gamma$, [46, 47] for $H \to \tau\tau$, [48, 49] for $H \to W^+W^-$, and [50, 51] for $H \to ZZ$.

4. Results

In our analysis we have used the Bayesian statistical approach. It has been implemented using the public package Bayesian Analysis Toolkit (BAT) [52]. Flat priors have been chosen for the parameters to be fitted. We consider only one Wilson coefficient at a time and fit it first to the EWPO and Higgs-boson observables separately, and then to the combination of both.

Our results are summarized in Table 2 where we show the 95% probability regions on the Wilson coefficients assuming the NP scale to be 1 TeV. It can be observed that except for O_{HWB} the Electroweak precision constraints are much stronger than the Higgs signal strength data for all the operators which contribute to the EWPO.

---

[4]We define the SM K-factor to be the ratio of the cross section

from the LHC Higgs Cross Section Working Group [43] to the leading order number obtained using Madgraph.

Coefficient	Only EW Λ [TeV]		Only Higgs Λ [TeV]		EW + Higgs Λ [TeV]	
	$C_i = -1$	$C_i = 1$	$C_i = -1$	$C_i = 1$	$C_i = -1$	$C_i = 1$
C_{HG}	--	--	11.4	12.3	11.4	12.3
C_{HW}	--	--	5.1	9.1	5.1	9.1
C_{HB}	--	--	9.6	17.2	9.6	17.2
C_{HWB}	11.1	18.4	12.5	7.1	12.6	15.9
C_{HD}	6.3	15.4	0.5	0.8	6.3	15.5
$C_{H\square}$	--	--	0.9	0.7	0.9	0.7
$C_{HL}^{(1)}$	14.8	9.2	--	--	14.8	9.2
$C_{HL}^{(3)}$	9.8	14.8	0.9	1.7	9.8	14.9
C_{He}	8.2	12.8	--	--	8.2	12.8
$C_{HQ}^{(1)}$	6.2	5.0	0.2	0.3	6.2	5.0
$C_{HQ}^{(3)}$	9.6	8.7	1.3	0.7	9.7	8.7
C_{Hu}	3.9	3.6	0.4	0.3	3.9	3.6
C_{Hd}	2.7	4.1	0.2	0.3	2.7	4.1
C_{Hud}	--	--	--	--	--	--
C_{eH}	--	--	3.8	6.4	3.8	6.4
C_{uH}	--	--	1.4	1.3	1.4	1.3
C_{dH}	--	--	3.7	3.6	3.7	3.6

Table 3: Lower bounds on the NP scale in TeV obtained by setting $C_i = \pm 1$.

The strong constraint on C_{HWB} from the Higgs data is due to its contribution to the Higgs decay to two photons which is loop suppressed in the SM. More precisely, the direct NP contribution to the $H\gamma\gamma$ vertex can be written as,

$$\mathcal{L}_{NP} \subset \frac{v}{\Lambda^2}(-c_W s_W C_{HWB} + s_W^2 C_{HW} + c_W^2 C_{HB}) F_{\mu\nu}F^{\mu\nu}H, \qquad (27)$$

which has to be compared with the SM vertex $c_\gamma \frac{\alpha_{em}}{8\pi v} F_{\mu\nu}F^{\mu\nu}H$ with $c_\gamma \approx -6.48$.

In Fig. 1 the posterior distribution of C_{HWB} is shown with only EWPO and only Higgs signal strength data. Eq. (27) also explains why the bounds on C_{HW} and C_{HB} are rather strong from the Higgs signal strength data. The tight constraint on the operator O_{HG} can also be understood in a similar way. It contributes to the Higgs-boson production through gluon fusion,

$$\mathcal{L}_{NP} \subset \frac{v}{\Lambda^2} C_{HG} G_{\mu\nu}^A G^{\mu\nu A} H, \qquad (28)$$

which should be compared to the SM contribution $\frac{\alpha_s}{12\pi v} G_{\mu\nu}^A G^{\mu\nu A} H$, where α_s is the chromomagnetic fine-structure constant.

The bounds on the dimension-6 operator coefficients in Table 2 can also be translated into bounds on the NP scale for fixed values of the coefficients. We show them in Table 3 for two values, $C_i = 1$ and $C_i = -1$.

A close look at the Table 3 will reveal that, assuming $C_i(\Lambda) = \pm 1$, the lower bound on the NP scale for one of the operators that is constrained only by the Higgs data ($C_{H\square}$) is less than 1 TeV. As this is close to the energy scale being probed at the LHC, the validity of such low bounds may be questionable.
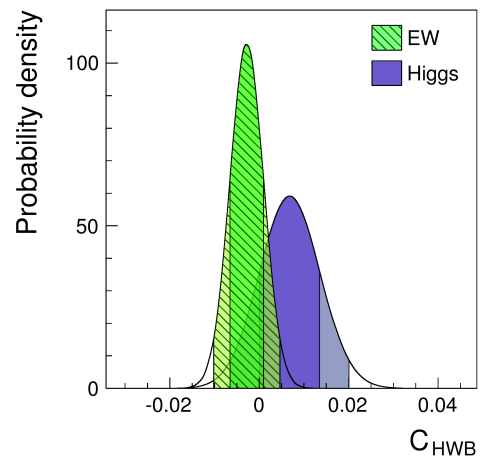

Figure 1: Posterior probabilities of C_{HWB} considering only the EWPO (green) and only Higgs signal strengths (blue). The dark and light regions are 68% and 95% probability regions respectively.

5. Conclusion

The discovery of a Higgs boson and the absence of any other direct signal of new physics motivates to adopt effective field theories to study possible deviations of the Higgs-boson couplings from the SM. In this work we have taken the above route to study the effects of dimension-6 operators in Higgs physics. To this end, we have considered EWPO from LEP and Tevatron, and Higgs signal strength date from the LHC to fit the coefficients of the NP operators. In general, in an Ultraviolet (UV) complete model several operators are generated with specific relations among their coefficients. However, given the state of our knowledge about UV physics, any theoretical bias is premature and considering definite combinations of the operators in a fit is not strongly motivated. Here we have studied only one NP operator at a time. Barring accidental cancellations, our results should provide an estimate of the bounds even in relatively general scenarios. Updated results including more than one operator at a time will be presented in a future publication [53].

The summary of our results is presented in Tables 2 and 3. It is interesting that there is a strong hierarchy among the lower bounds on NP scales of different operators. It spans from cases with ~ 1 TeV ($C_{H\square}$) to ~ 15-20 TeV (e.g., C_{HB}).

We observe that, except for the operator O_{HWB}, the Higgs strength data is redundant for all the operators which contribute to the EWPO. The bound from Higgs data for the operator O_{HWB} is comparable to that obtained from EWPO. However, there are also operators (e.g., $O_{HG,HW,HB}$) which are only constrained by the Higgs data. Moreover, as some of them contribute to loop-suppressed processes in the SM, the bounds on them are rather strong.

To summarize, the preliminary results presented here indicate that the NP scale is beyond the reach of LHC energy for most of the operators if the Wilson coefficients are assumed to be ± 1. However, these bounds can be weaker if the coefficients are smaller or specific correlations among the NP operators are present. Therefore NP scale of order $\sim$ TeV is allowed for perturbative values of the couplings.

Acknowledgments

References

[1] G. Aad, et al., Observation of a new particle in the search for the Standard Model Higgs boson with the ATLAS detector at the LHC, Phys.Lett. B716 (2012) 1–29. arXiv:1207.7214, doi:10.1016/j.physletb.2012.08.020.

[2] S. Chatrchyan, et al., Observation of a new boson at a mass of 125 GeV with the CMS experiment at the LHC, Phys.Lett. B716 (2012) 30–61. arXiv:1207.7235, doi:10.1016/j.physletb.2012.08.021.

[3] S. Weinberg, Baryon and Lepton Nonconserving Processes, Phys.Rev.Lett. 43 (1979) 1566–1570. doi:10.1103/PhysRevLett.43.1566.

[4] B. Grzadkowski, M. Iskrzynski, M. Misiak, J. Rosiek, Dimension-Six Terms in the Standard Model Lagrangian, JHEP 1010 (2010) 085. arXiv:1008.4884, doi:10.1007/JHEP10(2010)085.

[5] W. Buchmuller, D. Wyler, Effective Lagrangian Analysis of New Interactions and Flavor Conservation, Nucl.Phys. B268 (1986) 621–653. doi:10.1016/0550-3213(86)90262-2.

[6] R. Alonso, E. E. Jenkins, A. V. Manohar, M. Trott, Renormalization Group Evolution of the Standard Model Dimension Six Operators III: Gauge Coupling Dependence and Phenomenology, JHEP 1404 (2014) 159. arXiv:1312.2014, doi:10.1007/JHEP04(2014)159.

[7] Z. Han, W. Skiba, Effective theory analysis of precision electroweak data, Phys.Rev. D71 (2005) 075009. arXiv:hep-ph/0412166, doi:10.1103/PhysRevD.71.075009.

[8] F. del Aguila, J. de Blas, Electroweak constraints on new physics, Fortsch.Phys. 59 (2011) 1036–1040. arXiv:1105.6103, doi:10.1002/prop.201100068.

[9] D. Carmi, A. Falkowski, E. Kuflik, T. Volansky, J. Zupan, Higgs After the Discovery: A Status Report, JHEP 1210 (2012) 196. arXiv:1207.1718, doi:10.1007/JHEP10(2012)196.

[10] S. S. Biswal, R. M. Godbole, B. Mellado, S. Raychaudhuri, Azimuthal Angle Probe of Anomalous HWW Couplings at a High Energy ep Collider, Phys.Rev.Lett. 109 (2012) 261801. arXiv:1203.6285, doi:10.1103/PhysRevLett.109.261801.

[11] S. Banerjee, S. Mukhopadhyay, B. Mukhopadhyaya, New Higgs interactions and recent data from the LHC and the Tevatron, JHEP 1210 (2012) 062. arXiv:1207.3588, doi:10.1007/JHEP10(2012)062.

[12] T. Corbett, O. Eboli, J. Gonzalez-Fraile, M. Gonzalez-Garcia, Constraining anomalous Higgs interactions, Phys.Rev. D86 (2012) 075013. arXiv:1207.1344, doi:10.1103/PhysRevD.86.075013.

[13] T. Corbett, O. Eboli, J. Gonzalez-Fraile, M. Gonzalez-Garcia, Robust Determination of the Higgs Couplings: Power to the Data, Phys.Rev. D87 (2013) 015022. arXiv:1211.4580, doi:10.1103/PhysRevD.87.015022.

[14] E. Masso, V. Sanz, Limits on Anomalous Couplings of the Higgs to Electroweak Gauge Bosons from LEP and LHC, Phys.Rev. D87 (3) (2013) 033001. arXiv:1211.1320, doi:10.1103/PhysRevD.87.033001.

[15] D. Ghosh, R. Godbole, M. Guchait, K. Mohan, D. Sengupta, Looking for an Invisible Higgs Signal at the

LHC, Phys.Lett. B725 (2013) 344–351. arXiv:1211.7015, doi:10.1016/j.physletb.2013.07.042.

[16] B. Dumont, S. Fichet, G. von Gersdorff, A Bayesian view of the Higgs sector with higher dimensional operators, JHEP 1307 (2013) 065. arXiv:1304.3369, doi:10.1007/JHEP07(2013)065.

[17] M. B. Einhorn, J. Wudka, The Bases of Effective Field Theories, Nucl.Phys. B876 (2013) 556–574. arXiv:1307.0478, doi:10.1016/j.nuclphysb.2013.08.023.

[18] M. B. Einhorn, J. Wudka, Higgs-Boson Couplings Beyond the Standard Model, Nucl.Phys. B877 (2013) 792–806. arXiv:1308.2255, doi:10.1016/j.nuclphysb.2013.11.004.

[19] E. Boos, V. Bunichev, M. Dubinin, Y. Kurihara, Higgs boson signal at complete tree level in the SM extension by dimension-six operators, Phys.Rev. D89 (3) (2014) 035001. arXiv:1309.5410, doi:10.1103/PhysRevD.89.035001.

[20] E. E. Jenkins, A. V. Manohar, M. Trott, Renormalization Group Evolution of the Standard Model Dimension Six Operators I: Formalism and lambda Dependence, JHEP 1310 (2013) 087. arXiv:1308.2627, doi:10.1007/JHEP10(2013)087.

[21] E. E. Jenkins, A. V. Manohar, M. Trott, Renormalization Group Evolution of the Standard Model Dimension Six Operators II: Yukawa Dependence, JHEP 1401 (2014) 035. arXiv:1310.4838, doi:10.1007/JHEP01(2014)035.

[22] I. Brivio, T. Corbett, O. boli, M. Gavela, J. Gonzalez-Fraile, et al., Disentangling a dynamical Higgs, JHEP 1403 (2014) 024. arXiv:1311.1823, doi:10.1007/JHEP03(2014)024.

[23] C. Grojean, E. E. Jenkins, A. V. Manohar, M. Trott, Renormalization Group Scaling of Higgs Operators and $\Gamma(h \to \gamma\gamma)$, JHEP 1304 (2013) 016. arXiv:1301.2588, doi:10.1007/JHEP04(2013)016.

[24] R. Contino, M. Ghezzi, C. Grojean, M. Muhlleitner, M. Spira, Effective Lagrangian for a light Higgs-like scalar, JHEP 1307 (2013) 035. arXiv:1303.3876, doi:10.1007/JHEP07(2013)035.

[25] R. Contino, M. Ghezzi, C. Grojean, M. Muhlleitner, M. Spira, eHDECAY: an Implementation of the Higgs Effective Lagrangian into HDECAY, arXiv:1403.3381.

[26] A. Pomarol, F. Riva, Towards the Ultimate SM Fit to Close in on Higgs Physics, JHEP 1401 (2014) 151. arXiv:1308.2803, doi:10.1007/JHEP01(2014)151.

[27] A. Alloul, B. Fuks, V. Sanz, Phenomenology of the Higgs Effective Lagrangian via FEYNRULES, JHEP 1404 (2014) 110. arXiv:1310.5150, doi:10.1007/JHEP04(2014)110.

[28] M. Ciuchini, E. Franco, S. Mishima, L. Silvestrini, Electroweak Precision Observables, New Physics and the Nature of a 126 GeV Higgs Boson, JHEP 1308 (2013) 106. arXiv:1306.4644, doi:10.1007/JHEP08(2013)106.

[29] J. Elias-Mir, J. Espinosa, E. Masso, A. Pomarol, Renormalization of dimension-six operators relevant for the Higgs decays $h \to \gamma\gamma, \gamma Z$, JHEP 1308 (2013) 033. arXiv:1302.5661, doi:10.1007/JHEP08(2013)033.

[30] J. Elias-Miro, J. Espinosa, E. Masso, A. Pomarol, Higgs windows to new physics through d=6 operators: constraints and one-loop anomalous dimensions, JHEP 1311 (2013) 066. arXiv:1308.1879, doi:10.1007/JHEP11(2013)066.

[31] J. Elias-Mir, C. Grojean, R. S. Gupta, D. Marzocca, Scaling and tuning of EW and Higgs observables, JHEP 1405 (2014) 019. arXiv:1312.2928, doi:10.1007/JHEP05(2014)019.

[32] J. de Blas, Electroweak limits on physics beyond the Standard Model, EPJ Web Conf. 60 (2013) 19008. arXiv:1307.6173, doi:10.1051/epjconf/20136019008.

[33] J. Ellis, V. Sanz, T. You, Complete Higgs Sector Constraints on Dimension-6 Operators, JHEP 1407 (2014) 036. arXiv:1404.3667, doi:10.1007/JHEP07(2014)036.

[34] H. Belusca-Maito, Effective Higgs Lagrangian and Constraints on Higgs Couplings, arXiv:1404.5343.

[35] A. Biekoetter, A. Knochel, M. Kraemer, D. Liu, F. Riva, Vices and Virtues of Higgs EFTs at Large Energy, arXiv:1406.7320.

[36] M. Beneke, D. Boito, Y.-M. Wang, Anomalous Higgs couplings in angular asymmetries of $H \to Zl^+l^-$ and $e^+e^- \to HZ$, arXiv:1406.1361.

[37] K. Hagiwara, S. Ishihara, R. Szalapski, D. Zeppenfeld, Low-energy effects of new interactions in the electroweak boson sector, Phys.Rev. D48 (1993) 2182–2203. doi:10.1103/PhysRevD.48.2182.

[38] G. Giudice, C. Grojean, A. Pomarol, R. Rattazzi, The Strongly-Interacting Light Higgs, JHEP 0706 (2007) 045. arXiv:hep-ph/0703164, doi:10.1088/1126-6708/2007/06/045.

[39] M. E. Peskin, T. Takeuchi, A New constraint on a strongly interacting Higgs sector, Phys.Rev.Lett. 65 (1990) 964–967. doi:10.1103/PhysRevLett.65.964.

[40] S. Mishima, Update of the electroweak precision fit and model-independent constraints on new physics, Talk at ICHEP 2014, http://indico.ific.uv.es/indico/getFile.py/access?contribId=764&sessionId=30&resId=0&materialId=slides&confId=2025.

[41] A. Alloul, N. D. Christensen, C. Degrande, C. Duhr, B. Fuks, FeynRules 2.0 - A complete toolbox for tree-level phenomenology, Comput.Phys.Commun. 185 (2014) 2250–2300. arXiv:1310.1921, doi:10.1016/j.cpc.2014.04.012.

[42] J. Alwall, R. Frederix, S. Frixione, V. Hirschi, F. Maltoni, et al., The automated computation of tree-level and next-to-leading order differential cross sections, and their matching to parton shower simulations, JHEP 1407 (2014) 079. arXiv:1405.0301, doi:10.1007/JHEP07(2014)079.

[43] S. Heinemeyer, et al., Handbook of LHC Higgs Cross Sections: 3. Higgs PropertiesarXiv:1307.1347, doi:10.5170/CERN-2013-004.

[44] Measurements of the properties of the Higgs-like boson in the two photon decay channel with the ATLAS detector using 25 fb^{-1} of proton-proton collision data, Tech. Rep. ATLAS-CONF-2013-012, CERN, Geneva (Mar 2013).

[45] Updated measurements of the Higgs boson at 125 GeV in the two photon decay channel, Tech. Rep. CMS-PAS-HIG-13-001, CERN, Geneva (2013).

[46] Search for the Standard-Model Higgs boson decaying to tau pairs in proton-proton collisions at sqrt(s) = 7 and 8 TeV, Tech. Rep. CMS-PAS-HIG-13-004, CERN, Geneva (2013).

[47] Evidence for Higgs Boson Decays to the $\tau^+\tau^-$ Final State with the ATLAS Detector, Tech. Rep. ATLAS-CONF-2013-108, CERN, Geneva (Nov 2013).

[48] Measurements of the properties of the Higgs-like boson in the $WW^{(*)} \to \ell\nu\ell\nu$ decay channel with the ATLAS detector using 25 fb^{-1} of proton-proton collision data, Tech. Rep. ATLAS-CONF-2013-030, CERN, Geneva (Mar 2013).

[49] S. Chatrchyan, et al., Measurement of Higgs boson production and properties in the WW decay channel with leptonic final states, JHEP 1401 (2014) 096. arXiv:1312.1129, doi:10.1007/JHEP01(2014)096.

[50] Measurements of the properties of the Higgs-like boson in the four lepton decay channel with the ATLAS detector using 25 fb1 of proton-proton collision data, Tech. Rep. ATLAS-CONF-2013-013, CERN, Geneva (Mar 2013).

[51] Properties of the Higgs-like boson in the decay H to ZZ to 4l in pp collisions at sqrt s =7 and 8 TeV, Tech. Rep. CMS-PAS-HIG-13-002, CERN, Geneva (2013).

[52] A. Caldwell, D. Kollár, K. Kröninger, BAT - The Bayesian analysis toolkit, Computer Physics Communications 180 (2009) 2197–2209. arXiv:0808.2552, doi:10.1016/j.cpc.2009.06.026.

[53] J. de Blas, M. Ciuchini, E. Franco, D. Ghosh, S. Mishima, M. Pierini, L. Reina, L. Silvestrini, in preparation.